

# Vibrating polymeric microsieves: Antifouling strategies for microfiltration

Miriam Gironès i Nogué, Imam J. Akbarsyah, Lydia A.M. Bolhuis-Versteeg,  
Rob G.H. Lammertink\*, Matthias Wessling

Membrane Technology Group, University of Twente, Faculty of Science and Technology, P.O. Box 217, 7500 AE Enschede, The Netherlands

Received 7 June 2006; received in revised form 26 July 2006; accepted 3 September 2006

Available online 7 September 2006

## Abstract

Constant flux performance in time is achieved with polyethersulfone (PES) polymeric microsieves when filtering protein solutions, skimmed milk and white beer in combination with backpulsing. Such microsieves are fabricated by phase separation micromolding (PS $\mu$ M) and possess pores around 2  $\mu$ m. The filtration of bovine serum albumin (BSA) solutions at neutral pH results in constant flux when backpulsing. The constant flux performance is related to the ability of polymeric microsieves to flex during permeate pressure pulsing. Their flexibility allows pressure pulse transmission to the feed and, therefore, almost no flow reversal occurs. The membrane motion affects the hydrodynamics in the feed channel and disturbs the polarization layer and the cake deposited. Reference experiments with stiff Si<sub>x</sub>N<sub>y</sub>-based microsieves, nuclepore and macroporous microfiltration membranes show different behavior: the permeate pressure pulse hardly translates into the feed channel. Backpulsing for these membranes is less effect as anti-fouling strategy. Backpulsing of polymeric microsieves also allows stable flux operation for other complex feeds like skimmed milk and white Belgian beer.

© 2006 Elsevier B.V. All rights reserved.

**Keywords:** Microfiltration; Fouling; Microsieve; Beer; Milk; Protein solution

## 1. Introduction

Ceramic and polymeric membranes are nowadays used for the filtration of beer and dairy foods, replacing conventional Kieselguhr filtration or pasteurization. Crossflow microfiltration is currently used to remove bacteria from raw milk, separate casein from whey, and recover serum proteins from cheese whey, for instance [1–4]. In the brewing industry, current industrial crossflow microfiltration applications concern the clarification of rough beer to eliminate yeast and colloids responsible for haze, and sterile filtration of clarified beer.

Milk is a very complex fluid, mainly constituted by water and with a solid content around 12.6%. For the recovery of the milk protein fraction, skimmed milk is normally used as feed. Skimmed milk contains <0.5% (w/v) fat, 3.3% (w/v) proteins, 4.6–5.0% (w/v) lactose and minerals like calcium, sodium and potassium [4]. Fouling in skimmed milk filtration is normally associated to the protein fraction, formed by casein micelles and whey proteins like  $\beta$ -lactoglobulins,  $\alpha$ -

lactalbumins, immunoglobulins, bovine serum albumin (BSA), and others. Precipitation of calcium phosphates can also result in flux reduction. Currently used strategies to reduce fouling in milk filtration involve the use of backpulsing, acoustic or ultrasonic waves, turbulence promoters, vibrating and rotating disk modules and air sparging. A recent review of Brans et al. [3] has covered the state-of-the-art of these techniques and their possible disadvantages in milk fractionation. The differences between such strategies are their principle of operation, efficiency and costs. Turbulence promoters, vibration and rotating disk modules increase the shear rate close to the membrane, while backpulsing removes the cake layer by reversing the flow through the membrane. Air sparging reduces concentration polarization by mixing. Industrial implementation of these methods is very dependant on their efficiency (this at the same time depends on the feed and process parameters) and feasibility in terms of costs, upscaling and energy consumption.

Beer is a multi component feed, containing polysaccharides, higher dextrans and glucans, proteins and alcohols. The key membrane foulants in beer are proteins, carbohydrates ( $\beta$ -glucan, pentosan, etc.) and starch molecules or yeast cells. Crossflow microfiltration intends to replace conventional dead-end filtration with diatomaceous earth, for example. The main

\* Corresponding author. Tel.: +31 53 489 2063; fax: +31 53 489 4611.  
E-mail address: [r.g.h.lammertink@tnw.utwente.nl](mailto:r.g.h.lammertink@tnw.utwente.nl) (R.G.H. Lammertink).

components of beer to be removed during clarification are yeast cells and haze (polyphenols, proteins, carbohydrates and metal ions) [5]. To maximize the removal of chill haze, beer is normally filtered at 0 °C. This causes a flux limitation due to the increased solution viscosity. A number of mechanisms can be used to improve beer flux, including backpulsing or backflushing [6,7], flow pulsation, and oscillatory flow on the feed [8]. Together with backpulsing, the latter two are based on disturbing concentration polarization and the cake layer.

Today, commercially relevant fluxes in beer filtration are between 10 and 100 kg h<sup>-1</sup> m<sup>-2</sup> [6]. Microsieve membranes could very well supply the requirements needed for this application, because of their high flux and selectivity [9]. Currently, silicon nitride (Si<sub>x</sub>N<sub>y</sub>) microsieves are being introduced in dairy and brewing industry as a breakthrough technology. In spite of their advantages, there is still a trade-off associated with the high fluxes that such membranes can deliver: fouling. We have reported in previous work that fouling by proteins, for instance, can be reduced by several strategies such as backpulsing or antifouling coatings [10,11].

A new approach is being developed as an alternative to silicon nitride microsieves: polymeric microsieves. Microfiltration with novel polymeric microsieves represents a new technology with a viable potential for industrial implementation. These membranes exhibit similar selectivity/permeability characteristics to inorganic microsieves, but at much lower production costs. Due to the versatility of the fabrication process different pore sizes and shapes can be obtained [12–15]. Microsieves with pore diameters ranging from 5 μm (or higher) to approx. 0.5 μm are currently available [15]. Polymeric microsieves can deliver large product volumes operating at very low pressures, together with selective separations due to their precise pore size and shape.

Since polymeric microsieves are currently an emerging technology and no information about their performance in real filtrations is available yet, the outcome of the investigations in this article will serve as guidance for future applications. The main goal of this work is the evaluation of the filtration performance and fouling behavior of PES microsieves, using model protein solutions like BSA and real complex beverages like skimmed milk and beer. Polymeric microsieves with pore diameters of 2 μm have been selected as membranes for the fouling tests. Strategies like air sparging or backpulsing, which were extensively studied in previous research with Si<sub>x</sub>N<sub>y</sub> microsieves [10,11], have also been applied in order to enhance permeation. The backpulsing performance of polymeric microsieves in aqueous solutions will also be compared to other systems, like track-etched membranes and depth-filters.

## 2. Experimental

### 2.1. Materials

Microsieve PES membranes (pore size 5 and 2 μm) were used for the crossflow filtration of BSA solutions. For skimmed milk and beer filtration, 2 μm PES microsieves were used. The fabrication of such microsieves is discussed in detail in previous work [15]. For comparison, commercial track-etched membranes like

Nuclepore (polyethylene, 2 μm) and Millipore RAWP (cellulose esters, 1.2 μm) were used. Nuclepore membranes (low porosity) had a thickness of approx. 10 μm. Millipore RAWP had a porosity of 82% and an average thickness of 150 μm.

Ultrapure water (18.2 MΩ cm) for clean water flux measurements was obtained with a Millipore purification unit (MilliQ plus). BSA (Fraction V, Fluka) was used as model protein. The feed solutions consisted of 1 g/l BSA dissolved in filtered phosphate buffer 50 mM at pH 6.8 ± 0.1. Solutions were freshly prepared and stored at 8 °C for maximum 2 h before use. Commercially available sterilized skimmed milk (Euroshopper, pH 6.9–7) and white Belgian beer (Hoegaarden, pH 4.4) were used directly without any pre-treatment.

### 2.2. Crossflow microfiltration of BSA, skimmed milk and beer

The permeation experiments were performed in a cross-flow module with an effective membrane area of approx. 0.5 × 10<sup>-4</sup> m<sup>2</sup> and a channel height of 700 μm, shown in detail in previous work [9]. The microsieves and commercial membranes were glued onto a polymeric spacer acting as support (0.1 mm pore size) to enhance their mechanical strength, and then to a polysulfone sample holder which was inserted in the module.

Prior to the water flux measurements the membranes were inspected under an optical microscope to check their integrity. Subsequently, they were pre-wetted with water or a mixture of water and isopropanol. The clean water permeability was measured in the pressure range of 10–30 mbar at 20 ± 2 °C before any protein filtration.

BSA permeability was measured at a transmembrane pressure of approx. 18 mbar at 10 ± 2 °C, with an average crossflow velocity of 0.165 m/s. The filtrations of milk and beer were performed at approx. 10 ± 2 °C and an average operating pressure of 20 mbar. In all filtrations, the feed was stirred and pumped to the membrane module using a microannular pump with recirculation.

The influence of permeate backpulsing was studied with an electromagnetic backpulser (Aquamarijn Microfiltration B.V. [16]) described in previous work [10]. Variable frequencies and backpulsing power were applied in the backpulsing experiments with BSA solutions. Frequencies were varied from 2 to 6.7 Hz, power was varied from 30 to 50% of the maximum value and the pulse length was kept constant at 20 ms. In all experiments the tail was suppressed so that a symmetrical backpulsing profile was applied. Only in the case of the preliminary tests with the 2 μm microsieves a tail was applied (100 ms). For milk filtrations, the backpulse frequency was varied from 2.5 to 6.7 Hz at a constant pulse power and length (45% and 20 ms, respectively). White beer filtrations were performed at constant backpulsing frequency (4 Hz).

### 2.3. Scanning electron (SEM) and optical microscopy

The morphology of the microsieve membranes was visualized by scanning electron microscopy (SEM, Microscope JEOL

JSM-5600LV, at 5 kV). Quick microsieve inspection before and after the flux measurements was performed with an optical microscope (Zeiss Axiovert 40 MAT).

### 2.3.1. Analysis

The concentration of BSA and milk proteins in the feed and permeate was analyzed with a Cary 300 Scan UV–vis spectrophotometer at  $\lambda = 280$  nm. Single wavelength measurements were also performed to the beer feed and permeate fractions in the visible region, at  $\lambda = 450, 500, 600$  and  $800$  nm. The solid content of the fractions was determined by weight difference of evaporated samples with the same initial weight or volume. Samples were evaporated in a desiccator for 48 h and in a vacuum oven at  $30^\circ\text{C}$  for 5 days.

## 3. Results and discussion

### 3.1. Fouling studies with a model protein (BSA)

The average clean water permeability values of microsieves with  $5\ \mu\text{m}$  pore diameter varied between  $2$  and  $4 \times 10^6$  l/m<sup>2</sup> hbar. The scattering in these results originates from the differences in the intrinsic porosity, thickness difference among membranes and error in membrane area determination. From the SEM analysis performed in previous work [15] we can observe that, apart from the porosity introduced by perforation, additional intrinsic porosity created by the phase inversion method is present. Micropores in the unperforated zones may also contribute to such large fluxes.

When relatively stable BSA filtrations were analyzed we observed that flux decline took place to a great extent. This effect is displayed in Fig. 1A, where the relative BSA permeability of a  $5\ \mu\text{m}$  microsieve at pH 6.7 is shown in time. The surface morphology of such microsieve is shown in Fig. 1B. The filtration was performed at an operating pressure of  $21.5 \pm 1.5$  mbar. Permeability declined very rapidly in the first minutes of filtration, due to fast aggregate deposition, a phenomenon observed in former work for ceramic microsieves with  $1.2\ \mu\text{m}$  pore size [10]. The fact that BSA fouling or flux decline is usually associated to

aggregate deposition has been also confirmed by other authors in the past [17–19]. When air bubbles were introduced in the feed channel ( $t = 45$  min) permeability was slightly recovered because of partial aggregate removal from the membrane surface. This effect was confirmed previously in a former research with silicon nitride microsieves [11].

PES membranes have been extensively used by many authors to study fouling with BSA solutions [17,18,20,21]. Zeta-potential measurements on PES surfaces, reported by Pontié et al. [22] indicated that PES is negatively charged at neutral pH. Therefore, little electrostatic interactions between the membrane surface and the negatively charged BSA can occur. This reasoning and the findings of other authors [17,18,23,24], together with previous results obtained for inorganic microsieves [10] point thus to aggregate deposition as responsible mechanism for permeability loss for PES microsieves during BSA filtration.

From these observations it was clear that fouling is a critical aspect to be considered, even if microsieves with large pore sizes ( $5\ \mu\text{m}$ ) are used. Microsieves with  $5\ \mu\text{m}$  pores presented extremely large fluxes, which made it difficult to discriminate between flux anomalies caused by air, pressure changes or just protein fouling. That is why a more controllable system consisting of PES microsieves with an average pore size of  $2\ \mu\text{m}$  was chosen to study the fouling behavior of polymeric microsieves.

After a wetting step with a mixture of deionized water and isopropanol, clean water fluxes of thermally treated PES microsieves ( $250^\circ\text{C}$ , 60 min) with  $2\ \mu\text{m}$  average pore diameter (see Fig. 2) were measured. These membranes displayed an average water permeability of  $3.4 \times 10^5$  l/m<sup>2</sup> hbar, which is similar to the values obtained for Si<sub>x</sub>N<sub>y</sub> microsieves with pore sizes of about  $1.2\ \mu\text{m}$ .

The flow through a microsieve can be described by the Stokes flow, applicable at low Reynolds numbers. Van Rijn and coworkers [25,26] described the flow through short cylindrical channels with length  $L$  and diameter  $d$  by the following equation:

$$J = \frac{nd_{\text{pore}}^3 \Delta p}{24\mu A_m} \left[ 1 + \frac{16L}{3\pi d_{\text{pore}}} \right]^{-1} [1 - f(\varepsilon)]^{-1} \quad (1)$$

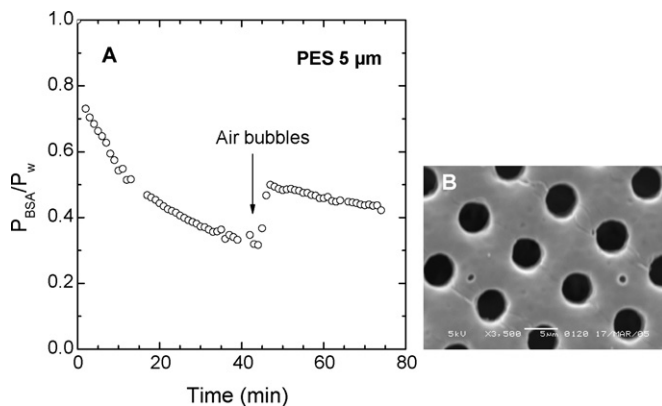


Fig. 1. (A) Flux decline vs. time of 1 g/l BSA pH 6.7 with a  $5\ \mu\text{m}$  PES microsieve at constant pressure ( $P_{\text{BSA}}/P_w = \text{BSA permeability/water permeability} = \text{relative BSA permeability}$ ). (B) The surface of such microsieve before filtration is displayed.

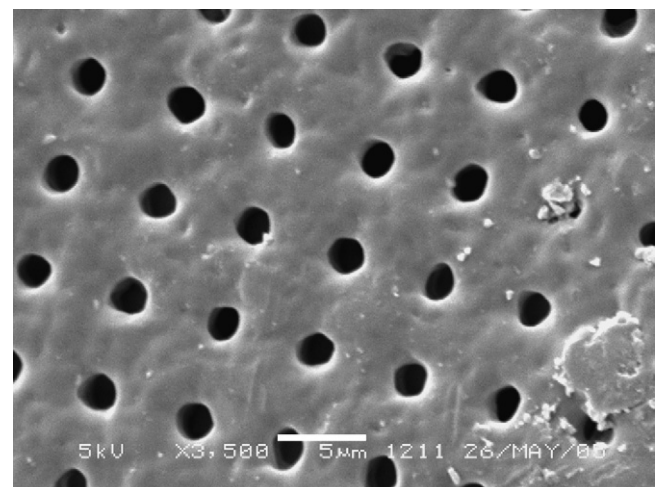


Fig. 2. Surface morphology of a PES microsieve with  $2\ \mu\text{m}$  pore diameter, fabricated by thermal treatment ( $250^\circ\text{C}$ , 60 min).

where  $n$  is the number of pores,  $L$  and  $d_{\text{pore}}$  the length and diameter of a pore, respectively,  $\Delta p$  the applied pressure,  $\mu$  the solution viscosity,  $A_m$  the membrane area and  $\varepsilon$  is the porosity. The porosity function  $f(\varepsilon)$  is defined as:

$$f(\varepsilon) = \sum_{i=1} a_i \varepsilon^{(2i+1)/2} \quad (2)$$

with  $a_1 = 0.894$ ,  $a_2 = 0.111$  and  $a_3 = 0.066$  [25]. For a polymeric PES microsieve with  $L = 8.5 \mu\text{m}$ ,  $d_{\text{pore}} = 2 \mu\text{m}$  and  $\varepsilon = 0.06$ , a permeability ( $J/\Delta p$ ) of about  $3 \times 10^5 \text{ l/m}^2 \text{ hbar}$  is obtained with this equation. The estimated permeability with the equation agrees quite nicely with the measured values.

Microsieves with perforations around  $2 \mu\text{m}$  were also used to investigate the flux decline of a 1 g/l BSA solution at pH 6.8 and  $31 \pm 1 \text{ mbar}$ . Fig. 3A shows how the membrane permeability decreased to 50% in the first 5 min of filtration. After 1 h the microsieve was completely blocked and no permeation was observed. The BSA retention of a shrunk PES microsieve after 20 min of filtration was approx. 4.5%. After approx. 40 min, retention increased to 6%. Fig. 3B displays blocked areas on a microsieve after use and flushing with water. It is clearly seen how some pores are completely covered by a thick protein layer. The previous results suggest that pore blocking is also the mechanism responsible for the severe BSA flux decline with membranes with large pore sizes such as 2 or  $5 \mu\text{m}$ . Bowen et al. [27] postulated that if the membrane possessed a narrow pore size distribution and if the pore size was smaller than the particle size, such as it happens in our case, complete blocking takes place in the initial stage of filtration. For this mechanism a relationship between the first and second derivatives of the permeated volume ( $V$ ) versus time ( $t$ ) exists:

$$\frac{d^2 t}{dV^2} = \alpha \left( \frac{dt}{dV} \right)^\beta \quad (3)$$

where  $\alpha$  and  $\beta$  are the parameters of the blocking filtration laws for constant pressure. Bowen et al. [27] derived values for  $\beta$  for different blocking models, 2 being the beta value when pore blocking causes flux decline. Beta is obtained by calculating the slope of the logarithmic expression of formula (3). For microsieves with  $2 \mu\text{m}$  perforations the best fit for the experimental data gives a beta value of  $2.35 \pm 0.11$ . This

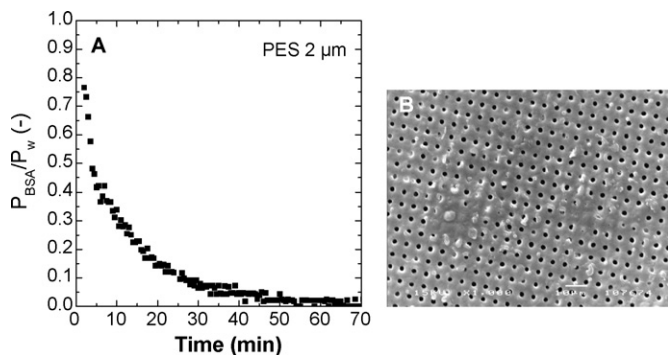


Fig. 3. Flux decline vs. time of 1 g/l BSA pH 6.8 with a  $2 \mu\text{m}$  PES microsieve (A), together with its surface morphology depicted with a SEM image after BSA filtration (B).

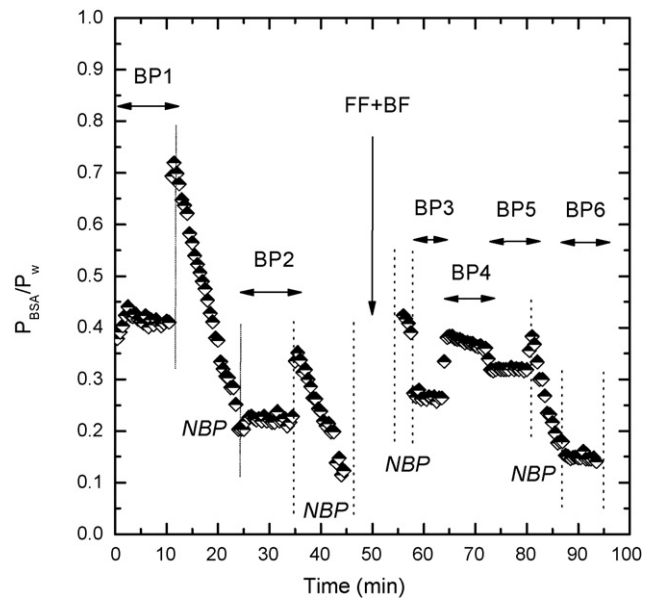


Fig. 4. Relative permeability vs. time of 1 mg/ml BSA pH 6.8 filtered through a  $2 \mu\text{m}$  at  $20^\circ\text{C}$ . The BP sections are the intervals where backpulsing was applied, during the NBP sections no backpulsing was applied. FF + BF stands for forward flushing and backflushing. The frequency (F) and the pulse length were kept constant at 6.7 Hz and 20 ms, respectively, while the power (P) and the tail settings (T) were varied.

clearly confirms the behavior predicted by the classical pore blockage model, even if the pore sizes used are large ( $2 \mu\text{m}$ ).

### 3.2. Fouling reduction strategies

Several strategies like backpulsing at variable frequency and power, forward flushing and backflushing were studied to reduce and retard fouling of BSA solutions at neutral pH. Water forward flushing consisted of injecting water discontinuously through the module inlet, whereas backflushing consisted of injecting water through the module permeate outlet.

The effectiveness of these methods was evaluated for a PES microsieve ( $2 \mu\text{m}$  pore diameter), and the outcome is shown in Fig. 4. Backpulsing frequency and power were kept constant throughout the experiment at 6.7 Hz and 30%, respectively, except for the BP5 and BP6 regions, where power was increased to 40%. Another variable was taken into account in the different regions: the tail or gradual descent of the backpulsing piston to the initial position. From BP1 to 3, a delay of 100 ms ( $T = 100 \text{ ms}$ ) was applied, whereas from BP4 onwards no delay was applied and the piston returned to its initial position immediately ( $T = 0 \text{ ms}$ ).

The results show that permeability remained constant when backpulsing was applied (BP1, BP2), even though a 60% loss in total permeability was observed initially in region BP1. Despite this fact, these results are very satisfactory, because for the first time constant permeabilities with BSA solutions were measured when backpulsing was applied. When backpulsing was stopped, a sudden increase of permeability was observed (due to reduced resistance offered by the backpulsing), until protein deposition occurred that caused permeability decline (NBP regions).



After 50 min of filtration, when only 10% of the permeability remained, water forward- and backflushing were applied. After reinitiating the filtration without backpulsing, permeability could be successfully but temporarily recovered up to 40% of its maximum value.

At BP3 reinitiation of backpulsing led again to constant permeability (25%, like in BP2). If the backpulsing tail was suppressed (BP4), an increase in permeability was observed, indicating that the pulse was more effective. But, since a slight flux decline occurred in this region (10%), backpulsing power was increased. This resulted in constant permeability (BP5). When backpulsing was stopped and then restarted with the same settings as in BP5, the same trend occurred as in the other intervals: first permeability declined and then it stabilized as backpulsing was activated (BP6).

The decrease in initial permeability when pulses are applied is a consequence of the pressure considered in our calculations. During a pulse, the average pressure at the permeate side is elevated and therefore the average flux is lower. In our case, only the operating pressure (average pressure at the feed side), which is normally constant and independent of backpulsing, is considered for the permeability calculation.

The pressure profiles exhibited in Fig. 5 demonstrate that PES microsieves act as pulse transmitters. First, when no membrane is present in the system (see Fig. 5A), we can observe that the feed pressure equals the permeate pressure, so the pulses are fully transmitted. From Fig. 5B and C it can be observed that the pulse is registered at the feed side when applied through a PES microsieve. During a pulse the feed pressure has almost the same value as the permeate pressure, resulting in almost no negative transmembrane pressure (TMP). In between pulses, feed pressure gradually increases until its set value (20 mbar). The peak value of the permeate pressure increases with the applied pulse power and results in more negative TMP values (see Fig. 5C).

In Fig. 6 the effect of the power and the pulse frequency at constant pulse power (45%) and length (20 ms) on the pulse profile is displayed. In all cases the pulse is clearly transmitted to the feed side, because  $p_{\text{feed}}$  is almost equal to  $p_{\text{permeate}}$ . In such case very little negative TMPs are reached, indicating that flow reversal is limited. An increase in pulse frequency results in less flux. Furthermore, at lower frequencies there is more time for the pressure to be stabilized before a pulse.

The previous results confirm that the fact that stable protein fluxes are obtained with BSA solutions is more likely to be caused by significant membrane motion rather than by a large backflow through the membrane. Mechanical motion was visually observed in our experiments during pulses and, furthermore, differences between feed and permeate pressure were low and only measured during a couple of ms for each pulse. Membrane motion can change fluid hydrodynamics on the membrane surface and decrease concentration polarization. Rodgers and Sparks [28] already reported this effect and postulated that membrane motion allowed an alteration of the solute concentration profile within the boundary layer so that the system concentration remains homogeneous during pulses.

Two approaches were applied to optimize backpulsing and increase membrane productivity. For the first one, the process

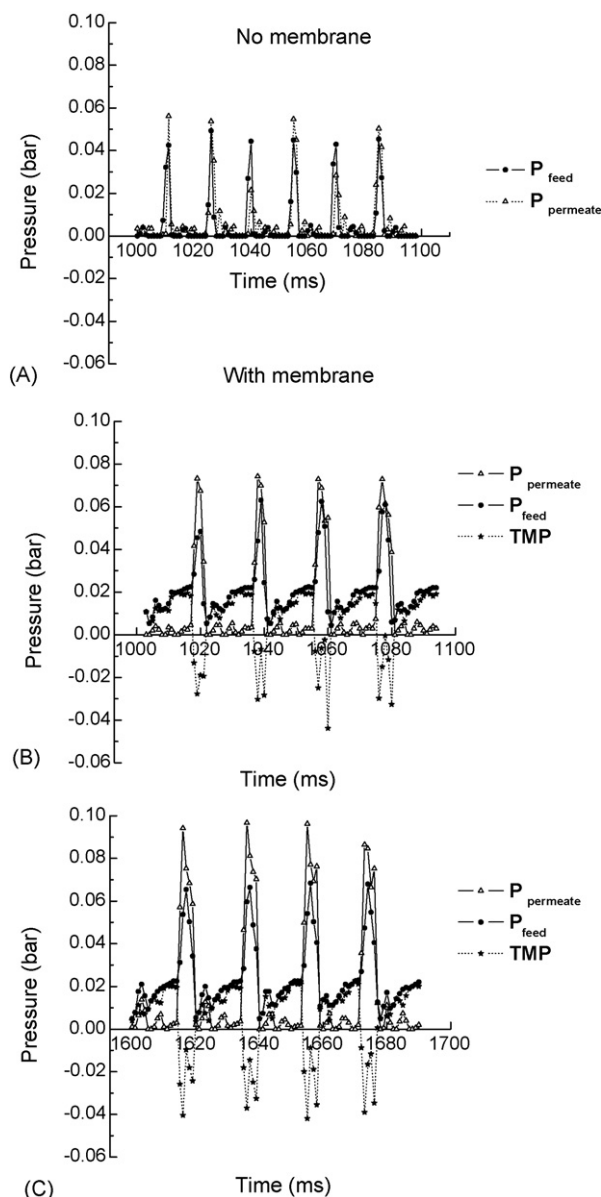


Fig. 5. Pressure as a function of time when backpulsing water (3.3 Hz, 20 ms) without membrane and 45% power (A) and with a PES microsieve at 45% (B) and 64% (C) power.

started without pulsing for a couple of minutes and then backpulsing was applied at high frequency (6.7 Hz), and regularly switched off for some seconds. Throughout the course of the experiment the frequency was varied as well. The outcome of this experimentation is presented in Fig. 7.

As already noted in Fig. 4, stopping the pulses for some seconds increased permeability for a short time only (see scattering in the data in the first set of experiments at 6.7 Hz). Lowering the frequency from 6.7 to 2.86 or 4 Hz resulted in an increase in permeability (approx. 10%) and constant permeation rate. Slightly rinsing the membrane with water did not increase permeability, probably because of little deposition on the surface. Relatively stable permeabilities (around 50%) were measured at intermediate pulse frequencies (2–4 Hz). After a non-pulsing period, backpulsing reinitiation at 2.86 Hz

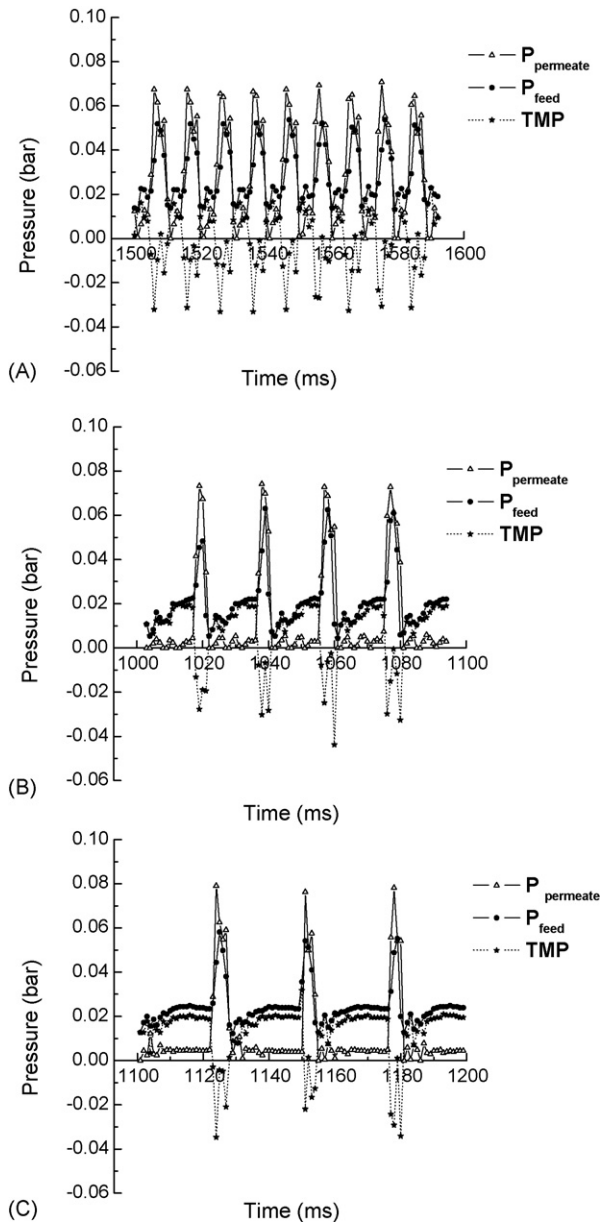


Fig. 6. Pulse profiles when backpulsing water at 45% power, 20 ms pulse and 6.7 Hz (A), 3.3 Hz (B) or 2.5 Hz (C), with a PES microsieve.

resulted in a constant permeability. Fairly constant permeability and enhancement were found when systematically stopping pulses and lowering the frequency.

Our second approach assumed that, if backpulsing would be initially started at lower frequencies, much higher permeability values might be obtained. A confirmation of this hypothesis is provided in Fig. 8. Backpulsing was initiated at 2.86 Hz and a relatively constant and high permeability was observed for the first time. A successive decrease of frequency increased the permeability even further. Then frequency was increased stepwise, from 2 to 2.86, 4 and 6.7 Hz. Once the frequency was increased, a decrease in permeability occurred, as expected. Fortunately, permeability could be increased in each regime by shortly stopping the pulses. The largest loss in BSA permeability (from 70 to 50%) occurred during the highest increase in frequency (from

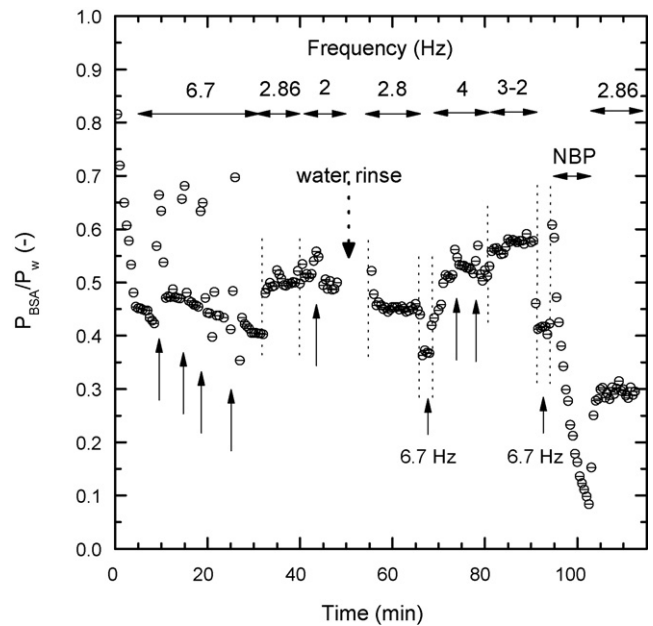


Fig. 7. Relative permeability vs. time of a BSA solution at pH 7 through a  $2\ \mu\text{m}$  PES microsieve. The arrows indicate the exact points where backpulsing was stopped and above the plot the different intervals with variable frequency are shown.

4 to 6.7 Hz), but it could easily be restored to the average value (70%) if frequency was lowered to 2.86 Hz. From these results, we can conclude that even though low frequencies are desirable for higher fluxes, flux decline is still slightly observed. At 4 Hz, though, a more stable flux is observed.

As observed in previous work with silicon nitride microsieves [11], air sparging at low air flows (10 ml/min) was also successful in stabilizing the permeation of BSA solutions through polymeric microsieves. Air sparging was applied for approx. 15 min

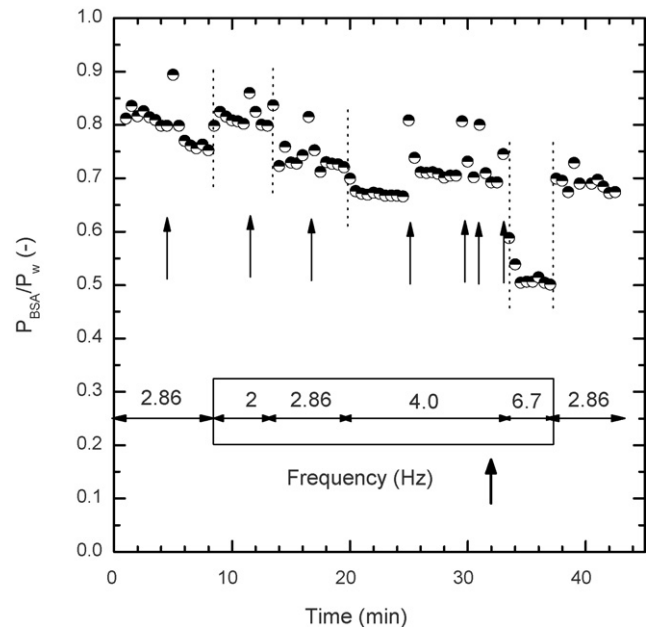


Fig. 8. Relative permeability vs. time of a BSA solution at pH 7 through a  $2\ \mu\text{m}$  PES microsieve. The arrows indicate the exact points where backpulsing was stopped.

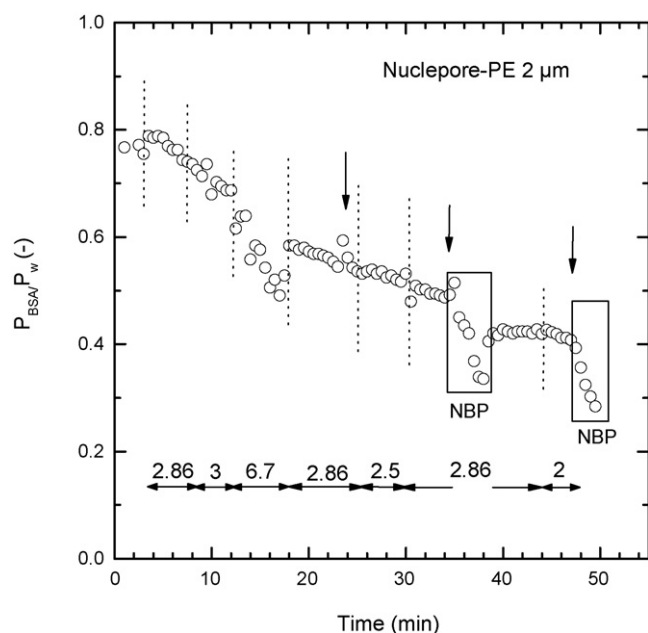


Fig. 9. Relative permeability vs. time of a BSA solution at pH 7.1 through a 2  $\mu\text{m}$  PE track-etched nuclepore membrane. The arrows indicate the exact points where backpulsing was stopped.

after the last backpulsing period in the experiment shown in Fig. 8. A stable constant flux was obtained, even though it was 40% lower than the last obtained value.

### 3.3. Comparison of polymeric microsieves and commercial membranes

From the previous section we can conclude that backpulsing BSA solutions at low frequencies is a very effective method to achieve stable fluxes with polymeric microsieves. In this situation, the determining factor in stabilizing permeability might be the mechanical motion of the microsieve during pulses. Such findings are a great breakthrough for microfiltration and potential applications of polymeric microsieves. In principle, this phenomenon might also be applicable to polymeric commercial screen filters, like track-etched membranes.

For comparison with current commercial systems, BSA was also filtered through Nuclepore track-etched membranes, with 2  $\mu\text{m}$  pore diameter and average clean water permeability of  $2 \times 10^5$  l/m<sup>2</sup> hbar. In Fig. 9 the outcome of a filtration experiment with BSA at pH 7.1 and backpulsing at different frequencies (20 ms pulse length, 45% power) is presented.

BSA permeability experienced decline even though backpulsing was applied. The most unfavorable conditions were obtained at high pulse frequencies, leading to flux instabilities and rapid decline. No backpulsing led to fast flux decline due to aggregate deposition. Initially, permeability did not remain constant for frequencies of 2.86–3 Hz, and declined even more at 6.7 Hz. After approx. 20 min the frequency was varied around 2.86–2.5 Hz and a gradual permeability decline of 10% was observed. When backpulsing was stopped for several minutes and restarted at 2.86 Hz, permeability stabilized at 40% of the maximum value.

In this experiment, even though the backpulsing settings were varied, permeability declined. Even successive pulse stops could not recover it. These results indicate that backpulsing a BSA solution was less effective for track-etched membranes than for microsieves, with these particular settings and solution properties. Direct comparison among these membranes in terms of BSA fouling should be done with caution, because even though their structures are rather similar in terms of thickness and pore design, the material properties, porosities and permeabilities are significantly different. More importantly, different surface–protein interactions may also occur depending on the membrane material. Therefore, it is difficult to establish if either adsorption, backpulsing inefficiency or reduced membrane motions are the causes for flux decline.

The pulse profiles with Nuclepore membranes, compared to PES microsieves are depicted in Fig. 10. For additional comparison, pulse profiles through a depth-filter Millipore RAWP and silicon nitride microsieves (both with pore diameter 1.2  $\mu\text{m}$ ) are also provided. The tests were performed with water, at a feed pressure of 20 mbar, constant frequency of 3.3 Hz, 45% power and a pulse length of 20 ms.

The main differences between the pulses through these membranes are the feed pressure profiles and corresponding TMP values. For the track-etched and the depth-filter membranes the profiles are very similar: the pulse is registered at the feed side, reaching a maximum value of approx. 35 mbar. The differences between backpulsing with such membranes and polymeric microsieves are striking. In the first place, considerably high feed pressures are measured with polymeric microsieves during a pulse, almost as high as the permeate pressure. This points out that the pulse is almost completely transmitted through the membrane and that only little permeate backflow exists. Nonetheless, backpulsing is very efficient because it can cause membrane motion and results in constant permeability.

Between pulses, the feed pressure also varied considerably (from 10 to 20 mbar). A pressure pulse is followed by a pressure dip, which is shown in the profile. The differences between silicon nitride and polymeric microsieves are even more obvious. The rigid membrane backstructure of Si<sub>x</sub>N<sub>y</sub> microsieves damps the pulse and very little pressure variations can be seen at the feed side. However, in this case there is indeed backtransport of permeate through the microsieve, because highly negative TMPs are recorded [10]. On the other hand, polymeric microsieves can experience motion (flexing) during pulses which enhance permeation. This is more likely to occur by such motion rather than by permeate flow reversal (flow reversal takes place but permeation in that direction is low).

### 3.4. Skimmed milk filtration

Skimmed milk was successfully filtered with a constant permeability around 20% of the maximum value when backpulsing was applied at constant operating pressure ( $20 \pm 2$  mbar) and variable frequency (see Fig. 11). Permeability reached a constant value independent of the pulse frequency. An exception can be observed at 6.7 Hz, where lower permeation was obtained.

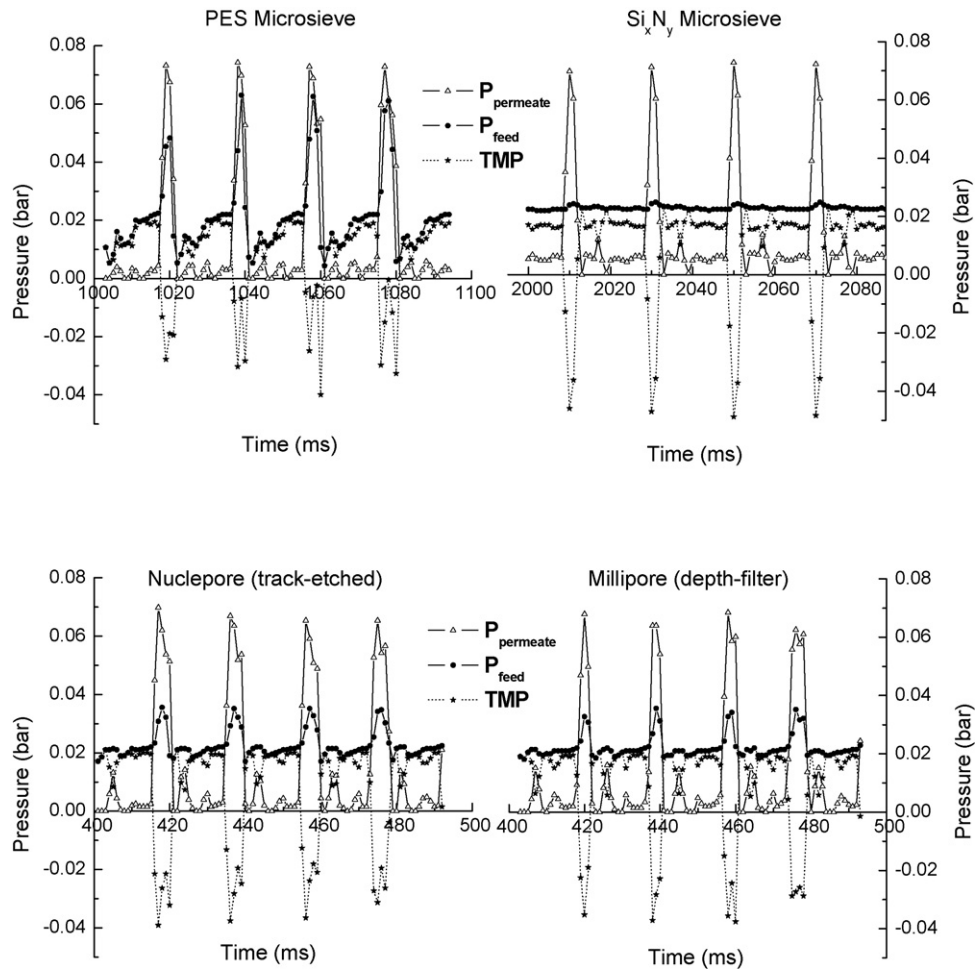


Fig. 10. Pulse profiles when backpulsing water (3.3 Hz, 45% power, 20 ms pulse) with a 2  $\mu\text{m}$  PES microsieve, 2  $\mu\text{m}$  nuclepore track-etched, 1.2  $\mu\text{m}$  silicon nitride microsieve and 1.2  $\mu\text{m}$  millipore depth-filter membrane.

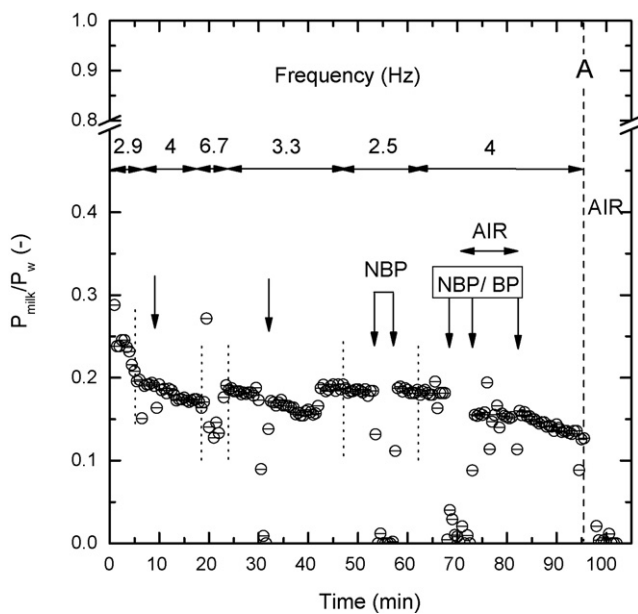


Fig. 11. Relative permeability of skimmed milk vs. time (pH 7, 9 °C), through a 2  $\mu\text{m}$  PES microsieve. The arrows indicate pulse stops for approx. 30 s; NBP indicates the regions where no pulses were applied for periods longer than 30 s.

When the pulses were stopped for a short period (minimum 30 s, indicated by the arrows), permeability did not increase (contrary to the results with BSA). Milk permeability decreased immediately and, if the pulses were suppressed for longer time, no permeate was obtained at all. Restarting the pulses with the same conditions successfully led to a permeability recovery to the last measured value. Such findings point to the fact that backpulsing is very effective in keeping the foulants fluidized above the membrane so that no deposition and further cake formation can occur.

As soon as pulsation was stopped, a cake layer from milk components such as casein micelles or whey proteins could settle down, thereby completely blocking the membrane surface. The deposited layer might be very compact, because flux descended to zero within a minute. In such case air sparging (12–20 ml/min) was not able to restore the flux (see Fig. 11,  $t = 70$  min). Mercier-Bonin et al. already reported low efficiency of two-phase flows in the enhancement of skimmed milk flux, during the separation of casein micelles from whey proteins [29,30], compared to the non-gas sparging situation. Moreover, this method is unlikely to be used in dairy food application, mainly because of foaming risks and protein damage.



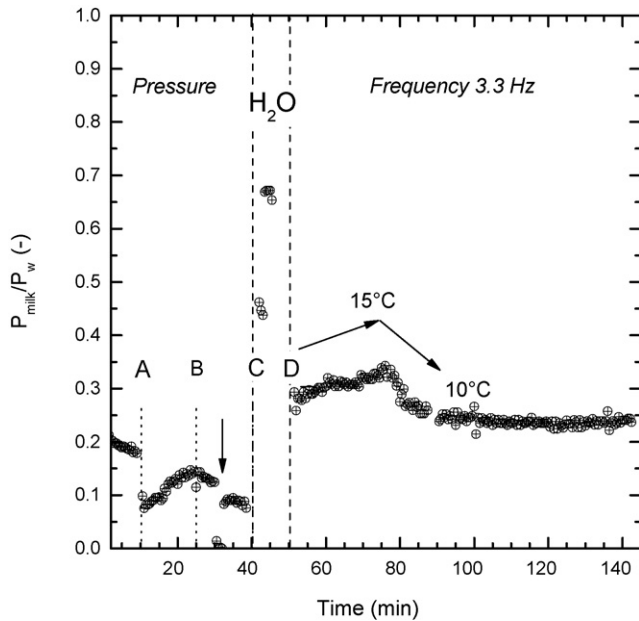


Fig. 12. Relative permeability of skimmed milk vs. time (pH 7, 7 °C), through a 2  $\mu\text{m}$  PES microsieve. From the initiation of the filtration until (C) pressure was successively varied. Until (A) pressure was 22 mbar, at (A) it was increased to 32 mbar for a minute, then decreased stepwise to 13.5 mbar until (B), where pressure was 16.4 mbar. During (B and C) pressure increased to 19 mbar after the pulse stop. At (C) forward and backflushing were applied, followed by feed exchange to water (C and D); from D to the end of the experiment milk was reintroduced as feed and the pressure and pulse frequency were kept constant (12 mbar, 3.3 Hz).

To confirm the reproducibility of the method, a longer experiment was performed for more than 2 h. The outcome of variable operating pressure on the milk permeability is shown in Fig. 12.

The filtration was initiated with backpulsing at 3 Hz and 22 mbar. At (A) the pressure was increased to 32 mbar and permeability suddenly dropped. After one minute, pressure was gradually lowered from 21 to 13.5 mbar (B), resulting in 50% permeability increase. From (B) until the pulses were stopped (indicated by the arrow) pressure was kept constant at 16.4 mbar, resulting in a stable flux, except when the pulses were suppressed. After backpulsing reinitiation, pressure was slightly increased until 19 mbar and permeability was constant for several minutes. At (C) water forward and backflushing were applied to rinse milk deposits, and the clean water flux was measured for 5 min. The rinsing step was proved to be very efficient, since the clean water permeability reached 70% of its maximum value. Such results also mean that little adhesion of the milk components on the microsieve surface occurs. After the forward and backflushing step, the pulsation of milk at 3.3 Hz and  $12 \pm 1$  mbar resulted in stable permeability for more than 90 min, with a flux of  $1600 \text{ l/m}^2 \text{ h}$ . The slight increase in milk permeability until  $t = 80$  min was probably caused by an increase in feed temperature to 15 °C. When the feed was rapidly cooled down to 10 °C permeability decreased to 27%, where it remained constant until the end of the test. A decrease of solution viscosity may have been the cause for the slight permeability increase ( $\eta_{\text{milk } 11^\circ\text{C}} = 2.1 \text{ mPa s}$ ,  $\eta_{\text{milk } 15^\circ\text{C}} = 1.84 \text{ mPa s}$ ).

Constant milk permeability was obtained in other tests when pressure was kept under 20 mbar and backpulsing frequency around 2.5 Hz.

Sterilized skimmed milk mainly contains lactose, casein, whey proteins and minerals like calcium. Fat is present as well, with a concentration  $< 0.5\%$ . Filtration of skimmed milk through 2  $\mu\text{m}$  PES microsieves could remove some of the remaining fat and some protein aggregates or casein micelles, which have normally mean diameters of 100 nm and are believed to form deposits on and inside the membrane pores [4]. During the course of the experiment, the absorbance of permeate samples was analyzed by spectrophotometry together with the feed at  $\lambda = 280 \text{ nm}$ , in order to detect differences in the total protein content. The same absorbance results were obtained at this wavelength, indicating that no protein was retained. The feed and permeate fractions collected during backpulsing had a very similar absorbance due to low concentration of the 'retainable' components (also at higher wavelengths than 280 nm).

With dynamic light scattering measurements no conclusive results could be obtained for the particle size of both feed and permeate fractions.

From the outcome of the milk filtration experiments, several recommendations can be made to optimize permeation and productivity. Backpulsing is necessary to avoid flux decline. Moreover, operating at relatively low frequencies and lower pressures permeation is enhanced. The use of air sparging with milk would not be recommended because it does not improve the permeation or flux recovery. More insight into retention and backpulsing influence might be gained by using semi-skimmed milk, which has a higher concentration of retainable components like fat globules.

### 3.5. White Belgian beer filtration

The white beer used as feed had certain turbidity characteristics, due to its yeast content. Our goal was to separate the largest suspended solid fraction and part of the yeast, which normally has sizes between 1 and 10  $\mu\text{m}$  [5]. The filtration of white beer at constant backpulsing frequency is shown in Fig. 13A. The same procedure and similar backpulsing settings were applied as with milk. When the feed was not degassed, large fluctuations in pressure occurred at the initial moments of filtration due to  $\text{CO}_2$ . However, once the system was free of gas stable operation was achieved.

After stabilization, backpulsing was initiated at 4 Hz. The pressure remained constant at an average value of  $18 \pm 1$  mbar for almost 1 h. Throughout this period, permeability was successfully stabilized and it remained constant just over 10% of its maximum. Pulses were suppressed twice (indicated by the arrows) resulting in immediate permeability loss. Restarting the pulses led to the same permeabilities than before the backpulsing stop, indicating that the deposited layer was removed. The average flux in the section shown in Fig. 13 was calculated to be  $1900 \text{ l/m}^2 \text{ h}$  (permeability around  $1 \times 10^5 \text{ l/m}^2 \text{ hbar}$ ).

After SEM inspection of the membrane surface, it was observed that some deposits were present in different zones.

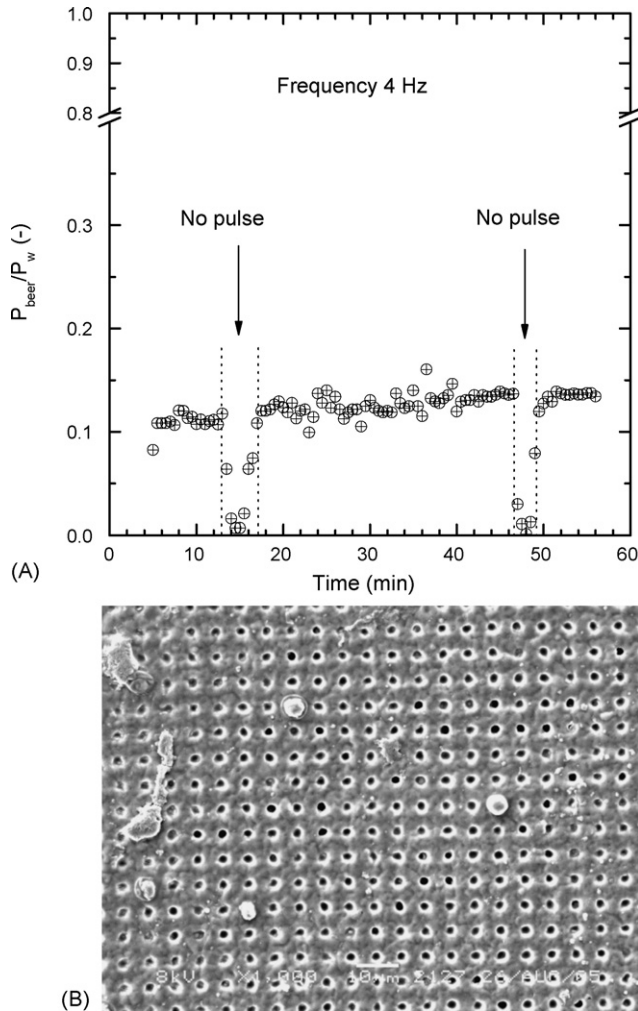


Fig. 13. (A) Relative beer permeability vs. time (13 °C), through a 2  $\mu\text{m}$  PES microsieve. During the filtration backpulsing was applied at constant frequency, power and pulse length (4 Hz, 45%, 20 ms). The operating pressure was  $18 \pm 1$  mbar. Backpulsing was stopped twice, indicated by the arrows. (B) SEM image of the microsieve surface after the white beer filtration.

However, the deposition was not extensive and most of the pores remained open for permeation, as shown in Fig. 13B.

After filtration, clear differences in turbidity were observed between the feed, retentate and permeate. The feed and permeate were analyzed with a UV–vis spectrophotometer at different wavelengths, between 450 and 800 nm. In Fig. 14, the differences in absorbance of the two fractions illustrate retention of beer particles that scatter light.

The temperature throughout the experiment was about 13 °C. Temperature has a very strong influence in beer filtration. Below 4 °C flocs of chill haze and other particles can sedimentate. This is important when these components are to be retained. According to Gan et al. [6], temperature also has an influence on the flux. Their experiments at 10 °C versus 2 °C, presented a higher beer flux but the permeate quality was reduced with respect to increased chill haze level. This effect was also observed in our different permeate fractions, which varied slightly in absorbance throughout the filtration. Those differences, though, were not

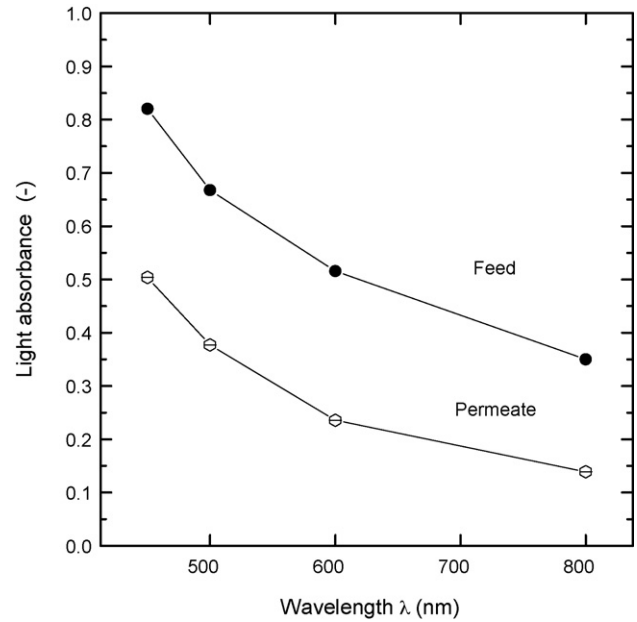


Fig. 14. Absorbance of the white beer feed and permeate vs. wavelength, directly after filtration through a 2  $\mu\text{m}$  PES microsieve.

significant compared to the feed, which presented much higher turbidity.

The retained solid fraction by the PES microsieves was determined by weight differences of evaporated samples. The solid fraction for the feed was determined to be 1.18 wt% and for the permeate 0.56 wt%.

#### 4. Conclusions

In this research the performance and fouling of 2  $\mu\text{m}$  PES microsieves, with a model protein like BSA, skimmed milk, and beer were investigated. For all cases, when no strategies like backpulsing were applied, severe and rapid flux decline took place, more acute for milk and beer than for BSA.

In the case of BSA, pore blocking by aggregate deposition was likely to be the determining mechanism behind flux decline, confirmed by the classical pore blocking theory. Since larger components were present in the other feeds, we also believe that the same mechanism may cause permeability loss in milk and beer filtrations.

From all fouling reduction strategies investigated in this work, backpulsing at low frequencies was the most successful method to enhance permeation, since it suppressed flux decline independently of the feed. Air sparging at low air flows (10 ml/min) was only applicable to BSA feed solutions in order to stabilize permeation rate. Air sparging in combination with milk was completely ineffective. Besides, little potential for this technique is available in dairy food processing, because of risk of foaming and protein damage. The highest permeabilities were achieved when backpulsing at low operating pressures with beer or milk.

The mechanism behind fouling reduction with polymeric microsieves and backpulsing is more likely to be mechanical motion of the membrane during pulsing rather than backflow.

Permeate pressure during pulsations is almost as high as feed pressure. This points out that the pulse is completely transmitted through the membrane and that very little permeate flow reversal exists. Enhanced permeation by microsieves motion represents an exceptional improvement, uncommonly seen for commercial systems.

Remarkably, the best performance with BSA as feed, in terms of backpulsing effectiveness and membrane productivity was achieved by using polymeric microsieves, when compared to commercial track-etched membranes and silicon nitride microsieves.

The average productivity of the PES microsieves presented in this chapter was found to be  $\geq 6000 \text{ l/m}^2 \text{ h}$  BSA,  $1600 \text{ l/m}^2 \text{ h}$  milk and  $1900 \text{ l/m}^2 \text{ h}$  of beer. These results are outstanding in comparison to conventional systems. For instance, a productivity of  $100 \text{ l/m}^2 \text{ h}$  beer is required for a membrane system to be implemented in industry. So, if microsieves with smaller pore sizes are fabricated, it is very likely that the process productivity will still be above average.

Due to their excellent filtration performance and the large fluxes obtained, microsieves can greatly change the membrane market for applications in dairy and brewing industry, but also other areas related to microfiltration.

## Acknowledgements

The authors would like to acknowledge the Dutch Ministries of Economic Affairs, Education, Culture and of Housing, Spatial Planning and Environment for the financial support (EET Program). Aquamarijn Microfiltration (Zutphen, The Netherlands) is acknowledged for the assembly and providing technical information about the backpulser. We mistakenly forgot to cite Ref. [16] in our previous paper [10] describing the effect of backpulsing. Maik Geerken is thanked for the assistance with the backpulsing profile measurements.

## References

- [1] M. Rosenberg, Current and future applications for membrane processes in the dairy industry, *Trends Food Sci. Technol.* 6 (1995) 12.
- [2] A.L. Zydney, Protein separations using membrane filtration: new opportunities for whey fractionation, *Int. Dairy J.* 8 (1998) 243.
- [3] G. Brans, C.G.P.H. Schroën, R.G.M. van der Smaan, R.M. Boom, Membrane fractionation of milk: state of the art and challenges, *J. Membr. Sci.* 243 (2004) 263.
- [4] A.D. Marshall, G. Daufin, Physico-chemical aspects of membrane fouling by dairy fluids, in: *Fouling and Cleaning in Pressure Driven Membrane Processes*, International Dairy Federation, Belgium, 1995.
- [5] L. Fillaudeau, H. Carrère, Yeast cells, beer composition and mean pore diameter impacts on fouling and retention during cross-flow filtration of beer with ceramic membranes, *J. Membr. Sci.* 196 (2002) 39.
- [6] Q. Gan, J.A. Howell, R.W. Field, R. England, M.R. Bird, C.L. O'Shaughnessy, M.T. McKechnie, Beer clarification by microfiltration—product quality control and fractionation of particles and macromolecules, *J. Membr. Sci.* 194 (2001) 185.
- [7] Q. Gan, Beer clarification by cross-flow microfiltration—effect of surface hydrodynamics and reversed membrane morphology, *Chem. Eng. Proc.* 40 (2001) 413.
- [8] P. Blanpain-Avet, N. Doubrovine, C. Lafforgue, M. Lalande, The effect of oscillatory flow on crossflow microfiltration of beer in a tubular mineral membrane system—membrane fouling resistance decrease and energetic considerations, *J. Membr. Sci.* 152 (1999) 151.
- [9] M. Gironès, R.G.H. Lammertink, Z. Borneman, M. Wessling, The role of wetting on the water flux performance of microsieves membranes, *J. Membr. Sci.* 259 (2005) 55.
- [10] M. Gironès, R.G.H. Lammertink, M. Wessling, Protein aggregate deposition and fouling reduction strategies with high-flux silicon nitride microsieves, *J. Membr. Sci.* 273 (2006) 68.
- [11] M. Gironès, L.A.M. Bolhuis-Versteeg, R.G.H. Lammertink, M. Wessling, Flux stabilization of silicon nitride microsieves by backpulsing and surface modification with PEG moieties, *J. Colloid Interf. Sci.* 299 (2006) 831.
- [12] C.J.M. van Rijn, L. Vogelaar, W. Nijdam, J.N. Barsema, M. Wessling, Method of making a product with a micro or nano sized structure and product, WO 0243937, 2002.
- [13] L. Vogelaar, J.N. Barsema, C.J.M. van Rijn, M. Wessling, Phase Separation Micromolding, *Adv. Mater.* 15 (2003) 1385.
- [14] L. Vogelaar, R.G.H. Lammertink, J.N. Barsema, W. Nijdam, L.A.M. Bolhuis-Versteeg, C.J.M. van Rijn, M. Wessling, Phase separation micro molding: a new generic approach towards microstructuring a wide range of materials, *Small* 1 (2005) 645.
- [15] M. Gironès, I.J. Akbarsyah, W. Nijdam, C.J.M. van Rijn, H.V. Jansen, R.G.H. Lammertink, M. Wessling, Polymeric microsieves produced by phase separation micromolding, *J. Membr. Sci.* 283 (2006) 411.
- [16] C.J.M. van Rijn, W. Nijdam, B.A.M. Mentink, Improving filter membrane performance, e.g. during cross-flow or dead-end filtration, involves delivering short back pulses to membrane during filtration, NL 1024292C, 2005.
- [17] S.T. Kelly, A.L. Zydney, Mechanisms for BSA fouling during microfiltration, *J. Membr. Sci.* 107 (1995) 115.
- [18] S.T. Kelly, W. Senyo Opong, A.L. Zydney, The influence of protein aggregates on the fouling of microfiltration membranes during stirred cell filtration, *J. Membr. Sci.* 80 (1993) 175.
- [19] C. Güell, R.H. Davis, Membrane fouling during microfiltration of protein mixtures, *J. Membr. Sci.* 119 (1996) 269.
- [20] C. Velasco, M. Ouammou, J.I. Calvo, A. Hernández, Protein fouling in microfiltration: deposition mechanism as a function of pressure for different pH, *J. Colloid Interf. Sci.* 266 (2003) 148.
- [21] J. Marchese, M. Ponce, N.A. Ochoa, P. Prádanos, L. Palacio, A. Hernández, Fouling behaviour of polyethersulfone UF membranes made with different PVP, *J. Membr. Sci.* 211 (2003) 1.
- [22] M. Pontié, X. Chasseray, D. Lemordant, J.M. Lainé, The streaming potential method for characterization of ultrafiltration organic membranes and the control of cleaning treatments, *J. Membr. Sci.* 129 (1997) 125.
- [23] G. Belfort, R.H. Davis, A.L. Zydney, The behavior of suspensions and macromolecular solutions in crossflow microfiltration, *J. Membr. Sci.* 95 (1994) 1.
- [24] S.T. Kelly, A.L. Zydney, Protein fouling during microfiltration: comparative behavior of different model proteins, *Biotechnol. Bioeng.* 55 (1997) 91.
- [25] S. Kuiper, C.J.M. Van Rijn, W. Nijdam, M.C. Elwenspoek, Development and applications of very high flux microfiltration membranes, *J. Membr. Sci.* 150 (1998) 1.
- [26] C.J.M. Van Rijn, M.C. Elwenspoek, Microfiltration membrane sieve with silicon micromachining for industrial and biomedical applications, in: *IEEE Proceedings MEMS*, Amsterdam, 1995.
- [27] W.R. Bowen, J.I. Calvo, A. Hernández, Steps of membrane blocking in flux decline during protein microfiltration, *J. Membr. Sci.* 101 (1995) 153.
- [28] V.G.J. Rodgers, R.E. Sparks, Effect of transmembrane pressure pulsing on concentration polarization, *J. Membr. Sci.* 68 (1992) 149.
- [29] M. Mercier-Bonin, C. Fonade, G. Gésan-Guiziu, Application of gas–liquid two-phase flows during crossflow microfiltration of skimmed milk under constant flux conditions, *Chem. Eng. Sci.* 59 (2004) 2333.
- [30] M. Mercier-Bonin, G. Gésan-Guiziu, C. Fonade, Application of gas–liquid two-phase flows during crossflow microfiltration of skimmed milk under constant transmembrane pressure conditions, *J. Membr. Sci.* 218 (2003) 93.